

External Calibration of Millimeter-Wave Atmospheric Radar Systems Using Corner Reflectors and Spheres

*M. Bergada, S. M. Sekelsky, and L. Li
Microwave Remote Sensing Laboratory
University of Massachusetts at Amherst
Amherst, Massachusetts*

Introduction

Millimeter-wave (MMW) radars have become standard cloud research tools because of their high sensitivity to small cloud particles, low prime power requirements, and compact size. However, MMW radars are more likely to suffer gain variations, so their calibration becomes crucial. Radar systems can be calibrated absolutely by various methods such as measurements of individual system parameters, comparison with in situ data, or external calibration using point targets. This paper focuses on this last method, which directly measures the combined response of all system components, and can be performed during a measurement campaign under field conditions.

In this paper, theoretical considerations are accompanied by calibration data obtained by the University of Massachusetts (UMass) Cloud Profiling Radar System (CPRS), a ground-based dual-wavelength MMW radar operating at 33 GHz and 95 GHz (Sekelsky 1996), during the Cloud Intensive Operational Period (IOP) 2000. The calibration was performed using triangular corner reflectors of two different sizes and metal spheres of three different sizes. The experimental setup and a comparison of the radar constants obtained with the different targets are discussed.

The Airborne Cloud Radar (ACR), an airborne-based 95 GHz radar (Sadowy 1999), was installed on the U.S. Department of Energy (DOE) Twin Otter during the ARESE II (Atmospheric Radiation Measurement [ARM] Enhanced Shortwave Experiment) experiment, which took place in Oklahoma at the same time as the Cloud IOP 2000. While mounted in the aircraft, ACR cannot be calibrated with the corner reflectors or spheres. Instead, ACR is calibrated by comparing zenith-pointing cloud measurements with those simultaneously measured by CPRS. In this manner, the CPRS calibration is transferred to ACR.

Calibration Constant from External Calibration Measurements

The calibration constant, R_c , relates measured power to radar reflectivity and accounts for all system parameters and for the dielectric constant of the hydrometeors (Battan 1973; Doviak et al. 1984; Smith 1986).

To perform an external calibration, calibration targets of a known radar cross section are measured (Ulaby et al. 1982). The measured power reflected from a calibration target, referenced to the input of the A-to-D converter, is described by

$$\bar{P}_{r(\text{ext-cal})} = \frac{P_t G_{\text{ant}}^2 \lambda^2 G_S \sigma_{\text{cal}}}{10^6 (4\pi)^3 L_{\text{tx}} L_r^2 R_{\text{cal}}^4} \text{ (mW)} \quad (1)$$

where σ_{cal} = the backscatter cross-section of the calibration target (m^2),
 l_{atm} = the one-way path integrated atmospheric loss between antenna and cal target, and
 R_{cal} = is the distance between the radar antenna and the cal target (km).

Thus, the following relationship gives us the value for the radar constant from the measurement of the received power from the cal target:

$$R_{c(\text{ext-cal})} = \frac{16 \ln 2 \lambda^4 \sigma_{\text{cal}} 10^{30}}{c \tau \theta^2 l_{\text{atm}}^2 R_{\text{cal}}^4 |K_w|^2 \bar{P}_{r(\text{ext-cal})}} \text{ (m/kW)}. \quad (2)$$

To simplify calibration, the distance between the radar and the calibration target must be larger than the far-field distance of the antenna ($R_{\text{cal}} > (2D^2/\lambda)$). However, the calibration target can be placed closer to the antenna if near-field approximations are performed. These are described in Sekelsky (2001).

The two-way extinction due to water vapor and oxygen from the radar antenna to the calibration target, l_{atm}^2 , can be removed if surface measurements of temperature, humidity, and pressure are available (Ulaby et al. 1982).

Calibration Targets: Triangular Trihedral Corner Reflector and Metal Sphere

The triangular trihedral is a widely used calibration target whose maximum backscatter cross section is described by:

$$\sigma_{\text{cr}} = \frac{\pi L^4}{3\lambda^2} \text{ (m}^2\text{)} \quad (3)$$

where L is the length of each of the three edges on the face of the reflector. Corner reflectors must be precisely machined for Eq. (3) to be applied. Error analysis (Robertson 1947) showed that a drop in excess of 5 dB in the level of σ_{max} results if one of the three angles of the corner reflector is 89 deg. instead of 90 deg.

The backscatter cross section of a perfectly conducting metal sphere is defined by Deirmendjian (1969):

$$\sigma_{\text{sphere}} = \pi r^2 \xi_b \quad (\text{m}^2) \quad (4)$$

where r is the radius of the sphere, and ξ_b is the backscatter efficiency of the metal sphere.

The size and radar cross section of the targets used in the calibration experiment are described in Table 1.

Table 1. Radar cross section of the calibration targets. L is the edge length of the corner reflector and r is the radius of the sphere.			
Target	Size (mm)	Ka-band (33 GHz)	W-band (95 GHz)
		$10 \log (s \text{ (m}^2))$	$10 \log (s \text{ (m}^2))$
Trihedral	$L = 107.8$	2.36	11.51
Trihedral	$L = 53.8$	-9.71	-0.56
Sphere	$r = 8.73$	-35.15	-36.45
Sphere	$r = 4.76$	-40.62	-40.89
Sphere	$r = 2.21$	-48.66	-48.63

CPRS Calibration: Experimental Setup and Results

The calibration experiment took place during spring of 2000, when CPRS was deployed at the Blackwell-Tonakawa airport, approximately 20 km from the DOE ARM Southern Great Plains (SGP) Cloud and Radiation Testbed (CART) site in Lamont, Oklahoma. The external calibrations were performed in an adjacent grassy field, using two portable towers of about 10 m in height, located 371 m and 727 m from CPRS. The towers are constructed from fiberglass and steel tubing. Guy points are located on slip rings so that the entire tower can be rotated to measure the radar cross section of the tower without tearing down the tower to remove the calibration target. The tower height is several times higher than the width of the radar footprint and when the corner reflector is mounted atop the tower, ground clutter reflections are avoided. However, the towers are not used to support the spheres because the radar cross section of the spheres is comparable to that of the tower. Instead, the spheres are launched across the radar beam using an air gun. Although tethered balloons with targets suspended below have been used in the past with mixed success, for narrow beam radars even light winds wreak havoc with the sphere's position and it's a constant struggle to align the target and radar beam. After some trial and error, it was determined that the best means of aligning the trajectory of the balls with the radar footprint is to launch the balls vertically across the beam at a fixed range. Both the radar temporal resolution and sphere velocity should be minimized so that the peak reflection that corresponds to the ball passing through the center of the radar beam is discerned. Although the tower is not used to support the sphere, it serves to align the azimuth angle of the beam with the trajectory of the sphere. The radar elevation angle is adjusted so that the center of the radar beam is located just below the apex of the sphere's trajectory, where the sphere's velocity is minimal. The air gun used for the experiment has a

nominal speed of 25 m/s. This means that the ball reaches 20 meters above the tower. The radar footprint was positioned somewhat lower than this height to account for variations in the air gun output. A schematic of the setup is shown in Figure 1.

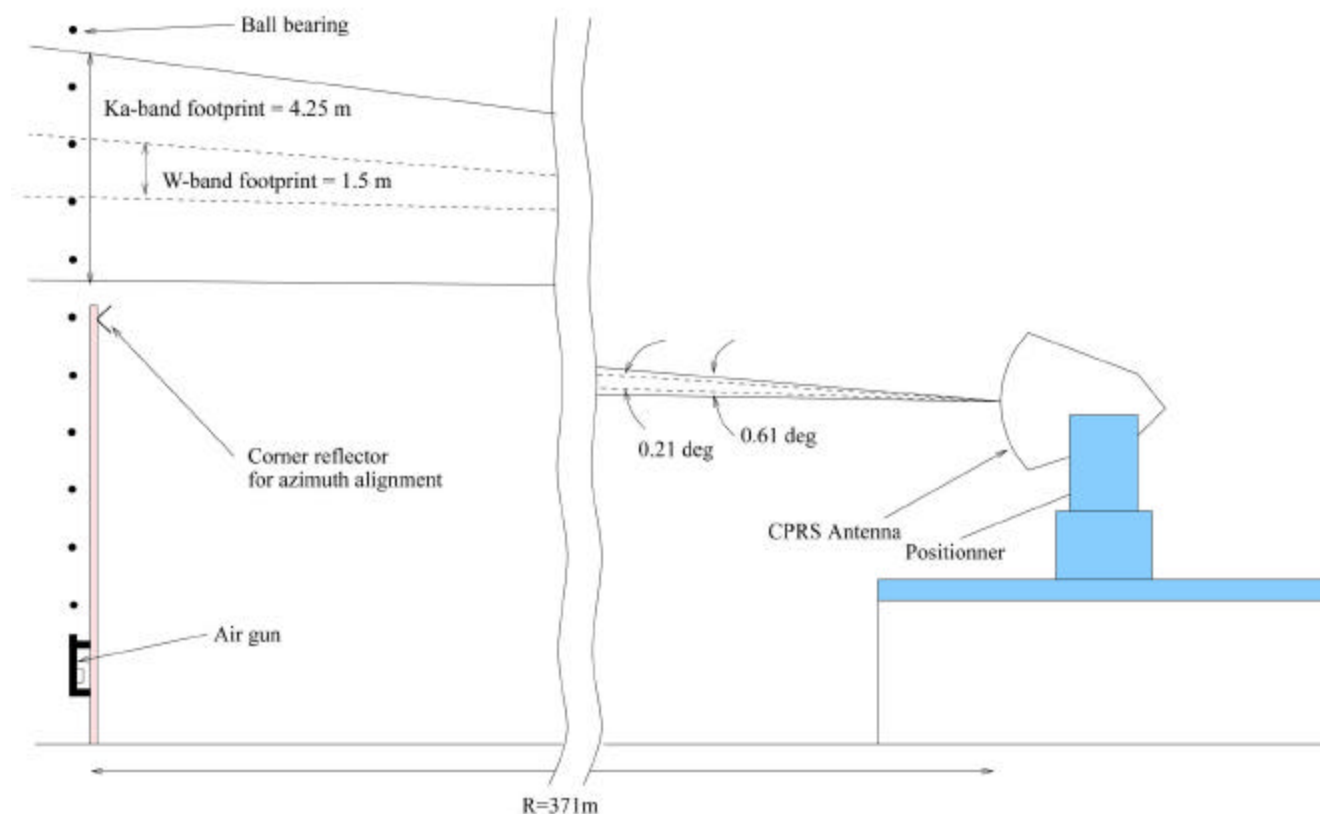
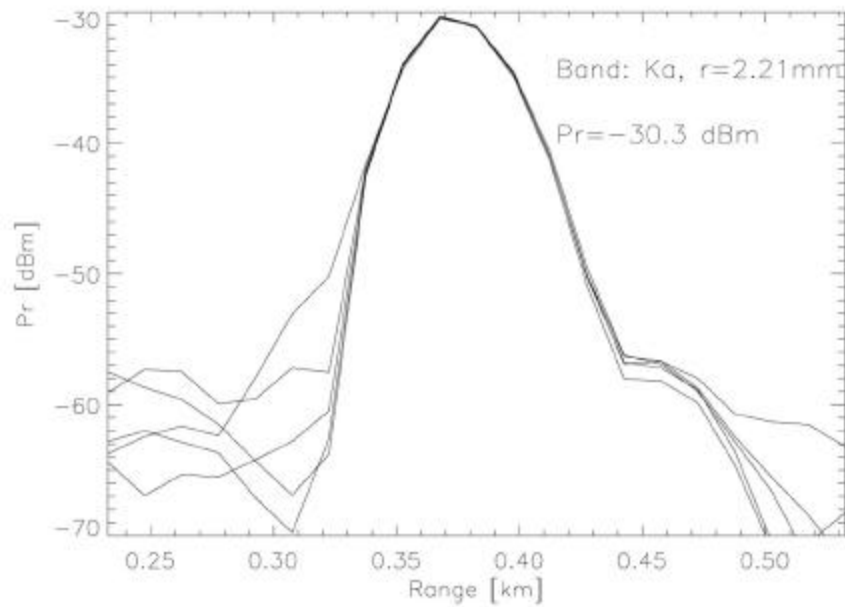


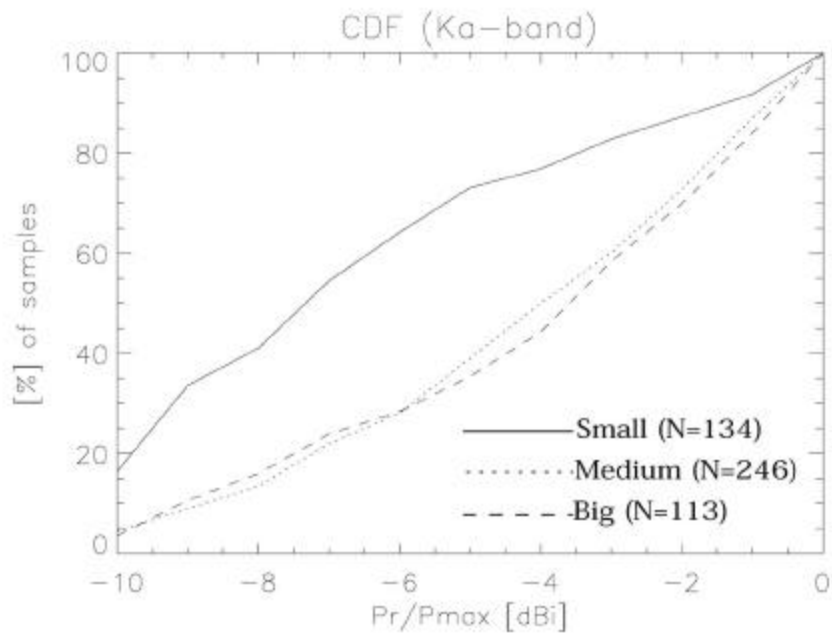
Figure 1. Experimental setup for the external calibration using metal spheres. The spheres are launched vertically from the base of the calibration tower.

A portable weather station located between CPRS and the first tower provides the temperature and humidity measurements used to determine the atmospheric absorption, which is almost negligible at Ka-band, while it's a little more important at W-band. To avoid insect clutter, calibrations were performed when ambient temperatures were low.

Figure 2(a) overplots the received power from the spheres' reflections for the small spheres ($r = 2.21\text{ mm}$) at Ka-band. However, only a small percentage of the shots are considered good, as can be seen in the CDF of Figure 2(b). This means that only a few spheres cross the center of the beamwidth. This is especially critical at W-band, where the beamwidth is even narrower, and for the smallest spheres. After retrieving the calibration constant obtained from the best sphere's shots, good agreement is achieved among the different size of spheres: $R_c = 35.99 \pm 0.28\text{ dB}$ at Ka-band and $R_c = 53.61 \pm 1.01\text{ dB}$ at W-band.



(a)



(b)

Figure 2. (a) Received power from the small sphere returns at Ka-band. Some of the shots that returned the maximum signal are overplotted. (b) CDF of the multiple shots for the three sizes of spheres at Ka-band, where N is the number of samples.

At Ka-band, the mean of R_c from all the corner reflector measurements is 36.01 dB, but there is a deviation of 3.70 dB from the maximum to the minimum values. For W-band, the mean is 52.60 dB and there is a spread of 2.05 dB. Some of the reasons for obtaining a little different calibration constants with different corner reflector measurements are the effect of clutter, especially significant at Ka-band; misalignment of the corner reflector; inaccuracy in the measurement of the Rx attenuator used to attenuate the strong echo from the corner reflector, which would saturate the receiver, and inaccuracy in determining the correct range of the target, since 15 m range gate spacing is used.

Transfer of CPRS Calibration to ACR

The ACR was mounted aboard the DOE Twin Otter during the ARESE II experiment. While mounted on the aircraft, ACR cannot be absolutely calibrated by means of the external calibration using point targets. Instead, it can be calibrated by intercomparison with the CPRS 95 GHz radar data while both radars are side-by-side, pointing towards zenith.

Such an experiment took place on March 9, 2000, in the Blackwell-Tonakawa airport. Figure 3 shows reflectivity data of a thin layer of clouds measured by both ACR and CPRS. Figure 4 displays one of the profiles. CPRS data is calibrated by means of the external calibration method and then transferred to ACR to match the profiles. ACR is continuously internally calibrated by means of an internal calibration loop, so only small corrections need to be applied to correct variations on the antenna gain. In Figure 4, both profiles match with an average error of less than 0.8 dB.

Summary

This paper presents the radar calibration of the UMass MMW radars performed during spring of 2000. Point targets calibration was used successfully to calibrate CPRS, using corner reflectors and spheres as calibration targets. Spheres proved to work better at Ka-band while corner reflector measurements were more stable at W-band. Then, side-by-side zenith pointing measurements of clouds allowed CPRS calibration to be transferred to ACR.

References

- Battan, L. J., 1973: *Radar observations of the atmosphere*. The University of Chicago Press, Chicago, Illinois.
- Deirmendjian, D., 1969: *Electromagnetic scattering on spherical polydispersions*. American Elsevier Publishing Co., Inc.
- Doviak, R. J., and D. S. Zrnic, 1984: *Doppler radar and weather observations*. Academic Press, Inc.
- Robertson, S. D., 1947: Targets for microwave radar navigation. *Bell System Tech., J.*, **26**, 852-869.

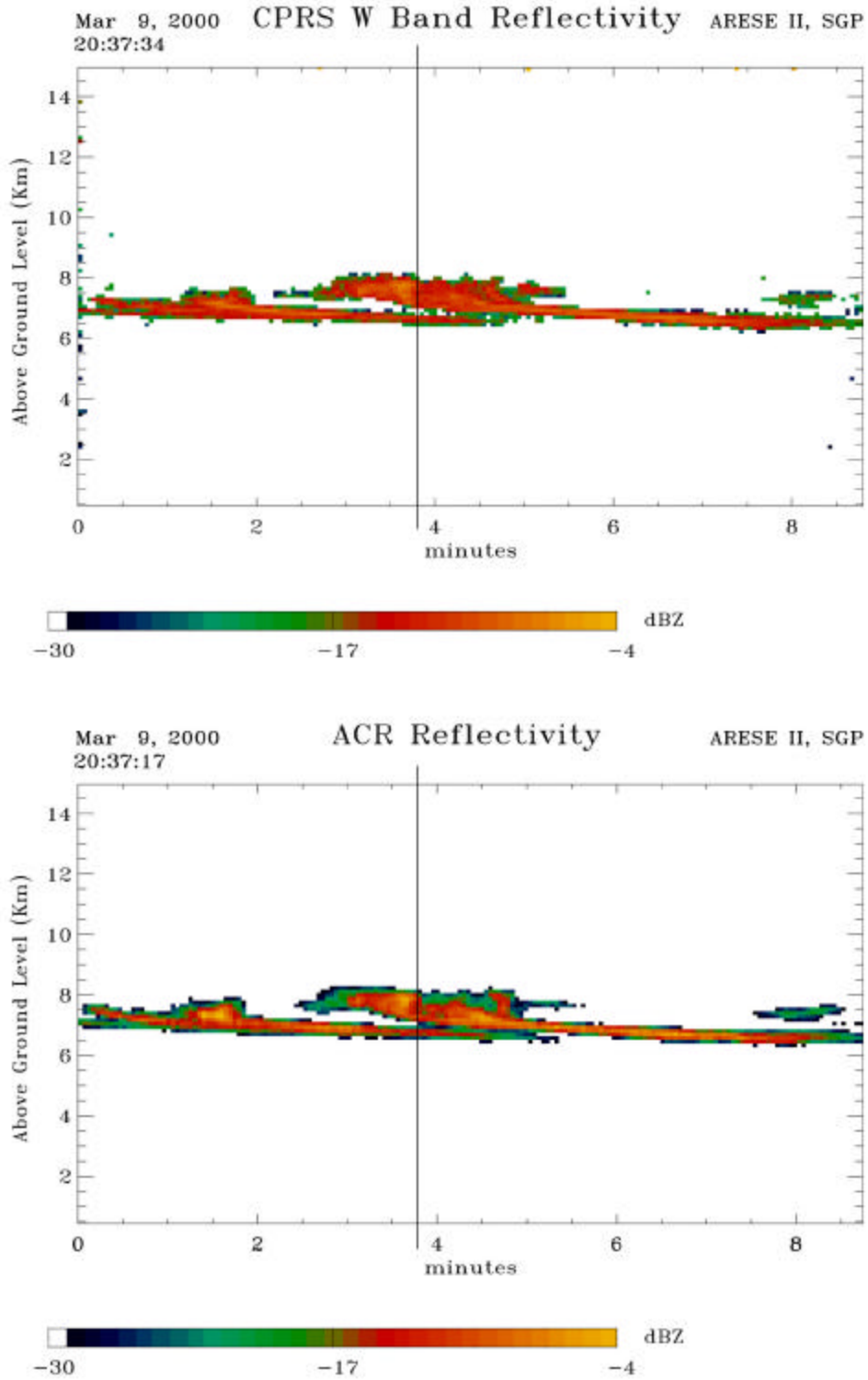


Figure 3. CPRS (top) and ACR (bottom) 95 GHz radar reflectivity of a thin layer of clouds, measured on March 9, 2000, during the Cloud IOP 2000 and ARESE II experiments.

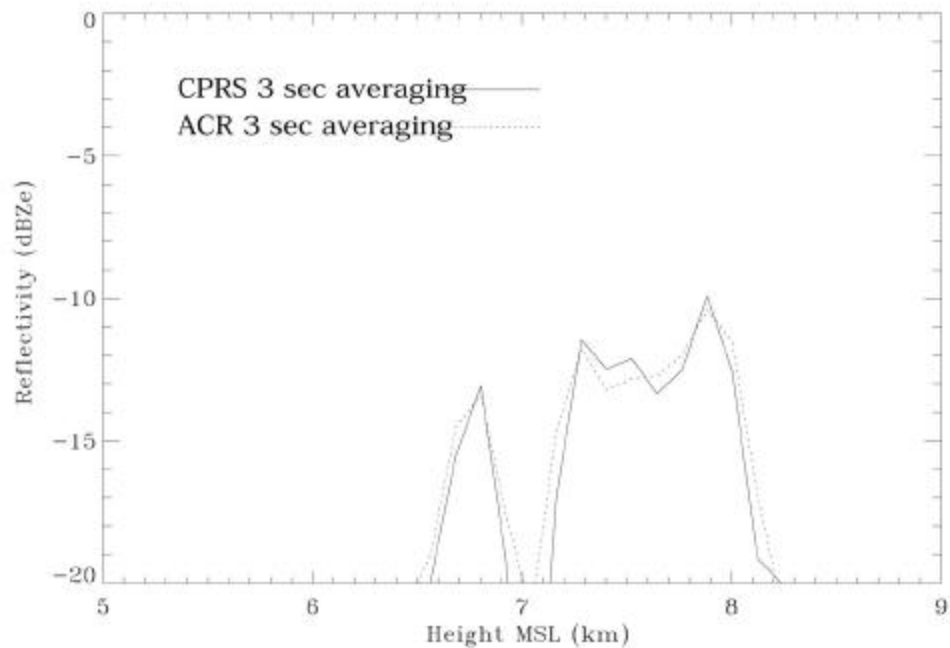


Figure 4. Intercomparison of ACR and CPRS 95 GHz radar reflectivity profile.

Sadowy, G., 1999: A 95 GHz cloud radar: Statistics of cloud reflectivity and analysis of beam-filling errors for a proposed spaceborne cloud radar. Ph.D. thesis, University of Massachusetts, Amherst, Massachusetts.

Sekelsky, S., 2001: Near-field corrections for millimeter-wave atmospheric radars. *J. Atmos. Oc. Tech.* Submitted.

Sekelsky, S., and R. McIntosh, 1996: Cloud observations with a polarimetric 33 GHz and 95 GHz radar. *Meteorology and Atmospheric Physics*, **58**, 123-140.

Smith, P. L., 1986: On the sensitivity of weather radars. *J. Atmos. Oc. Tech.*, **3**, 704-713.

Ulaby, F., R. Moore, and A. Fung, 1982: *Microwave remote sensing; active and passive, Vol. 1*. Artech House, Norwood, Massachusetts.